Chapter 16
Innovative Treatment Modalities for Craniofacial Reconstruction

Vasudev Vivekanand Nayak, Daniel Boczar, Paulo G. Coelho, Andrea Torroni, Christopher M. Runyan, James C. Melville, Simon Young, Bruce Cronstein, Roberto L. Flores, and Lukasz Witek

V. V. Nayak
Department of Biochemistry and Molecular Biology, University of Miami Miller School of Medicine, New York, NY, USA
e-mail: vxn188@miami.edu

D. Boczar
Department of Surgery, University of Washington, Seattle, WA, USA
e-mail: Boczad01@uw.edu

P. G. Coelho
Department of Biochemistry and Molecular Biology, University of Miami Miller School of Medicine, Miami, FL, USA

Division of Plastic Surgery, Department of Surgery, University of Miami Miller School of Medicine, Miami, FL, USA
e-mail: pgc51@med.miami.edu

A. Torroni · R. L. Flores
Hansjörg Wyss Department of Plastic Surgery, NYU Grossman School of Medicine, New York, NY, USA
e-mail: andrea.torroni@nyumc.org; roberto.Flores@nyulangone.org

C. M. Runyan
Department of Plastic Surgery, Wake Forest University School of Medicine, Winston-Salem, NC, USA
e-mail: crunyan@wakehealth.edu

J. C. Melville · S. Young
Bernard and Gloria Pepper Katz Department of Oral and Maxillofacial Surgery, School of Dentistry, The University of Texas Health Science Center at Houston, Houston, TX, USA
e-mail: James.C.Melville@uth.tmc.edu; Simon.Young@uth.tmc.edu

B. Cronstein
Department of Medicine, NYU Grossman School of Medicine, New York, NY, USA
e-mail: bruce.cronstein@nyumc.org

L. Witek (✉)
Biomaterials Division, NYU College of Dentistry, New York, NY, USA

Hansjörg Wyss Department of Plastic Surgery, NYU Grossman School of Medicine, New York, NY, USA

Department of Biomedical Engineering, NYU Tandon School of Engineering, Brooklyn, NY, USA
e-mail: lukasz.witek@nyu.edu

J. C. Melville et al. (eds.), *Advancements and Innovations in OMFS, ENT, and Facial Plastic Surgery*, https://doi.org/10.1007/978-3-031-32099-6_16

Introduction

The craniomaxillofacial (CMF) region is comprised of a complex system of soft and hard tissues. The primary function of the intracranial space is to accommodate the brain, while the oral cavity, which is anatomically encompassed by the cranial base and the mandible, enables respiration, speech, and mastication [1, 2]. Defects affecting this musculoskeletal structure of the midface comprise a large number of cases requiring CMF surgery. In the year 2020, 256,085 maxillofacial surgeries, 35,387 head and neck reconstructions, and 68,915 reconstructive surgeries were performed to address congenital deformities [3].

Cleft palate (e.g., anterior alveolar defect of the maxilla) has been reported to affect 1 in 600 newborns [4] and requires alveolar bone grafting traditionally harvested from the iliac crest. Hemifacial microsomia (HFM) and Pierre Robin sequence are both associated with micrognathia, which may cause tongue-based airway obstruction, and are often treated with mandibular distraction osteogenesis, requiring two separate operations with morbidities including facial scarring and potential nerve damage. Treacher Collins syndrome is another disorder associated with congenital absence of the zygoma necessitating autologous bone grafting. Craniosynostosis is a condition involving premature fusion of the cranial sutures that may lead to increased intracranial pressure. If left untreated, patients can potentially suffer from developmental delays or intellectual disabilities, malocclusion, dysphagia, and speech abnormalities [5]. Treatment modalities for this condition include cranial expansion surgery requiring autologous split cranial bone graft or autograft (native tissue) to adequately expand the skull without leaving critical size defects [6].

For many CMF bony defects, autografts, to date, are considered the "gold standard" reconstructive modality. Although an effective treatment modality, autografts are associated with multiple disadvantages including a limited quantity of available donor tissue, donor site morbidity, and the potential for infection at the site of surgery, along with cost [7]. Specifically, cleft repair with harvested autogenous iliac crest has been known to cause short- and long-term donor site pain and sensory disturbances [8]. HFM treatment using autogenous grafting procedures typically entails longer surgical procedures, greater surgical mobility, and asymmetry between the reconstructed side and the normal, unoperated, contralateral side [9]. Reconstructive surgery in the case of Treacher Collins syndrome involves using calvarial bone grafts, especially for zygomatic reconstruction. One primary limitation of this treatment modality is the resorption of the bone graft, seen in a majority of patients [10, 11]. Furthermore in the case of craniosynostosis treatment, the likely presence of critically sized defects necessitates the use of devices, grafts, and implants, to aid in the healing process [12].

A requirement for grafts or implants used in the reconstruction of CMF defects is the capacity to restore the bony defect while maintaining the three-dimensional (3D) skeletal architecture. Thus, the field of CMF surgery has evolved toward utilization of customized treatment plans for patients to improve outcomes in terms of

physiology, function, and aesthetics, post-recovery. Such challenges have warranted the search for alternative materials and modalities that are not limited in quantity, are biocompatible, have the capacity to be tailored specific to the patient and anatomic location, and are augmented with biologic factors to facilitate bone regeneration. This chapter focuses on the re-purposing of bulk materials that have been previously utilized for bony defect regeneration through the application of additive manufacturing techniques to advance CMF reconstruction in both pediatric and adult patients.

New Materials and Methods

Ceramics are synthesized solid inorganic materials that are crystalline in nature. Bioceramics are a subset of this class, which are biocompatible, bioinert, bioactive, or bioresorbable. Calcium phosphate (CaP)-based materials have garnered increased attention dating back to the early 1960s as they can be utilized as resorbable and implantable devices/materials in their bulk form [13–18]. CaP-based ceramics have a reliable safety profile and excellent biocompatibility [5]. Among the different CaP ceramics available, β-tricalcium phosphate (β-TCP) ($Ca_3(PO_4)_2$) and hydroxyapatite (HA) ($Ca_{10}(PO_4)_6(OH)_2$) have been widely utilized for bony defect regeneration [19]. Devices manufactured using HA or β-TCP have traditionally been fabricated through molding or casting. The process involves using a die to produce parts for a specific application. While the accuracy of parts generated remains satisfactory, the process is laborious to carry out for each patient or anatomic location requiring a customized, fit-and-fill graft. Furthermore, casting a part with controlled pore spacing and distribution is difficult, especially in small scaffolds. Such limitations have prompted the search for alternative manufacturing techniques that can more readily facilitate the production of patient-specific devices.

In the most recent form of additive manufacturing, 3D printing (3DP)—the sequential layer-by-layer addition of material, custom medical devices/scaffolds have been designed and fabricated using computer-aided design (CAD). While this form of rapid prototyping has evolved considerably in recent years in various surgical fields, its presence in CMF surgery has demonstrated substantially greater advances. One reason for such growth has been attributed to the paucity of clinically available patient-specific tissue engineering-based therapies [4]. Further advances in 3DP technology have been due to increased accuracy and stability of printed materials by simultaneously reducing post-processing steps required prior to implantation. Additive manufacturing (AM) of metals and polymers are relatively older techniques, whereas 3DP of ceramics through solid free-form fabrication (SFFF) or robocasting, is a newer and emerging method to fabricate resorbable, porous scaffolds through the use of ceramic-based slurries [20]. HA and β-TCP are two such CaP-based ceramics that can be extruded in a controlled fashion [21]. In their bulk form, both materials exhibit valuable biocompatibility and osseoconduction in vivo. HA, which is the primary inorganic component of bone, has been

reported to show ~2% resorption annually [22]. Such low resorption kinetics have rendered HA unfavorable in terms of a resorbable grafting material. β-TCP on the other hand has been shown to fully resorb within a period between 6 and 18 months depending on various factors (i.e., volume, shape, porosity, and surface characteristics) of the construct [23]. This has driven researchers to develop new workflows using β-TCP slurries to produce 3DP customized fit-and-fill scaffolds.

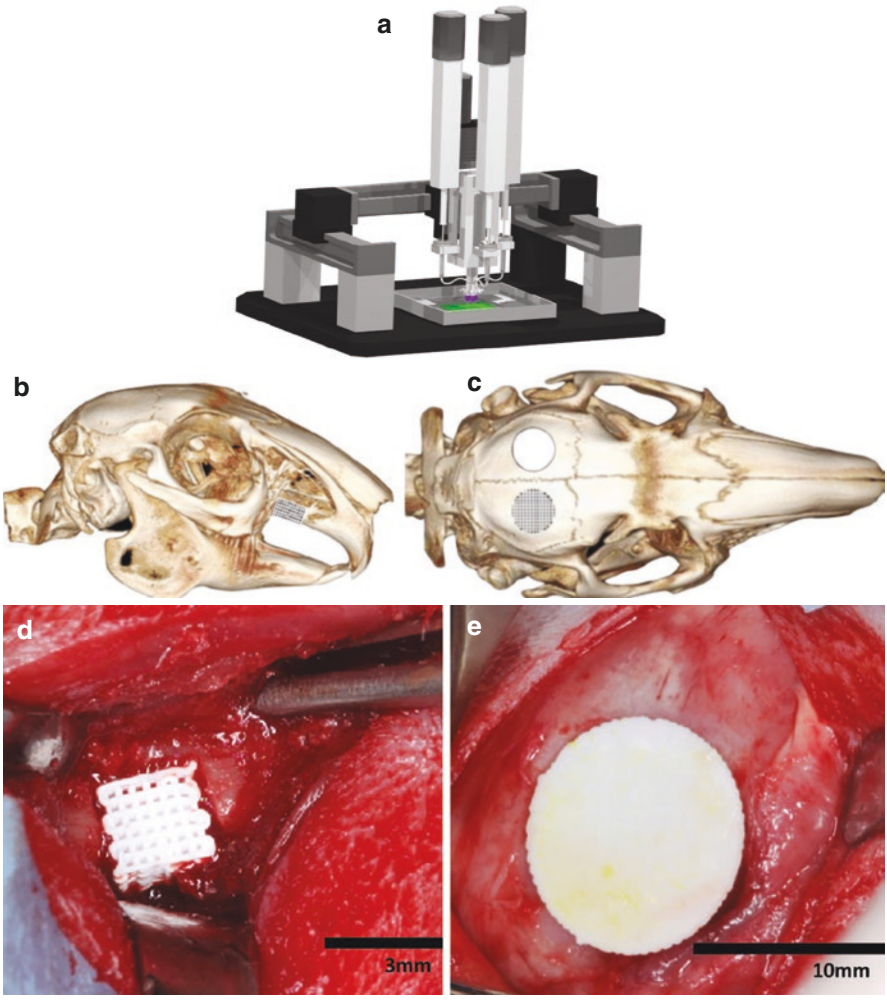

Fig. 16.1 (**a**) CAD rendering of custom-built solid free-form fabrication 3D printer. (**b**) Schematic depicting alveolar cleft model. (**c**) Schematic depicting calvarial defect model, intraoperative image of fit-and-fill reconstruction of (**d**) cleft and (**e**) calvarial defect with scaffold. (Reproduced with permission from Shen C, Wang MM, Witek L, Tovar N, Cronstein BN, Torroni A, et al. Transforming the Degradation Rate of β-tricalcium Phosphate Bone Replacement Using 3-Dimensional Printing. Annals of Plastic Surgery. 2021;87(6))

The 3D printing workflow for ceramics is multifaceted consisting of the following steps (Fig. 16.1):

1. *Pre-processing:* This step includes computer-aided design (CAD) and successive computer-aided manufacturing (CAM) to generate digital part files. With the introduction of 3D printing, CAD has seen significant development with its synergistic integration to hardware like micro-computed tomography (microCT) and volumetric rendering software tools such as AMIRA or mimics for isolation and refinement of the region of interest. The digitally reconstructed 3D computer-generated solid is then exported to stereolithography (.STL) format through discretization after which is it digitally sliced and meshed into a multilayered three-dimensional (3D) object. This slicing process converts the surface data of the .STL file into machine level ".gcode" comprising of coordinate-related instructions along with auxiliary commands such as feed rate, print speed, etc. This is especially useful to tailor the scaffold lattice parameters, namely, pore spacing, layer height, and rod size. Once the details have been set, the ".gcode" is exported to the SFFF printer.
2. *Printing:* SFFF printers consist of a stationary platform equipped with a moveable gantry. Commonly these printers consist of multiple extrusion nozzles to deposit both primary and secondary, fugitive support materials simultaneously. While there are various protocols published in the literature to synthesize a colloidal mixture or slurry of β-TCP, a previously established protocol combines powdered β-TCP powder with controlled amounts of antiflocculants, dispersive agents, and viscosifiers to generate a shear thinning gel [5, 21, 24]. The extruders of the SFFF printer follow a tool path in the *x*-, *y*-, and *z*-axes from the file while depositing the colloidal gel onto a substrate.
3. *Post-processing:* This type of fabrication method requires a single post-processing step. Ceramics are generally brittle without heat treatment, causing problems with handling and usage. To overcome this, ceramic scaffolds are heat treated (sintered) to solidify the constructs. The heating leads to shrinkage and subsequent densification of the construct for it to achieve the required mechanical properties for surgical handling. Subsequently, prior to implantation scaffolds are also sterilized in an autoclave at approximately 121°C before surgical implantation.

Bioactive Molecules (rhBMP-2, Adenosine, and Dipyridamole)

With the introduction of tissue engineering-based approaches, the embryonic process of tissue generation has been further recapitulated using mesenchymal stem cells (MSCs), growth factors (GFs), and cytokines [25–27]. Similarly, the unique combination of 3D-printed grafting materials and bioactive molecules can further enhance the rate of bone formation and regeneration, potentially reducing the time needed to return to form and function. Such results are possible due to increased osteoblast activity and subsequent reduction in osteoclast activity while also leading to scaffold resorption [4]. One such innovation that has resulted from the amalgamation of various surgical techniques is the use of recombinant human bone

morphogenetic protein-2 (rhBMP-2) for the reconstruction of segmental CMF defects [28].

Bone regeneration is a complex process with a primary goal being osseoinduction [4]. Recombinant human bone morphogenetic protein-2 (rhBMP-2) is one commercially available FDA-approved osteogenic agent. Its use in preclinical in vivo models has shown considerably faster bone regeneration when compared to scaffolds implanted without such bioactive molecules. Unfortunately, its share of drawbacks such as ectopic bone formation and premature suture fusion [29–34] has limited its use. In contrast, adenosine, commonly termed "the retaliatory metabolite," has gained popularity as an osteogenic agent capable of promoting higher levels of bone regeneration. The mechanism of action of adenosine is by attenuating activity of a wide array of cell types as a protective mechanism [35, 36]. Regulatory effects of adenosine such as induced protective vasodilatory and negative inotropic effects on stressed cardiac vessels and tissue have been reported for over a century [7]. While tissues are stressed, adenosine is present in higher quantities (e.g., in septic patients [35]). Adenosine receptors A_1 (ligation of which plays a role in osteoclast formation), A_{2A} (activation of which inhibits osteoclastogenesis), A_{2B} (agonism of which influences osteogenic differentiation), and A_{3A} (agonism of which has been reported to cause downregulation in bone resorption) cause systemic effects since they are present throughout almost every tissue [7]. However, in unstressed tissues, its activity is limited by its lower extracellular presence (~1 μM/L) and short half-life due to the aforementioned receptors being left inactivated even with continuous blockage of adenosine deaminase enzyme [19, 35].

Due to these shortcomings, the search for alternatives mainly through pharmacological manipulation has led research groups to the selection of dipyridamole (DIPY) as a suitable bioactive molecule. DIPY has been FDA approved for clinical

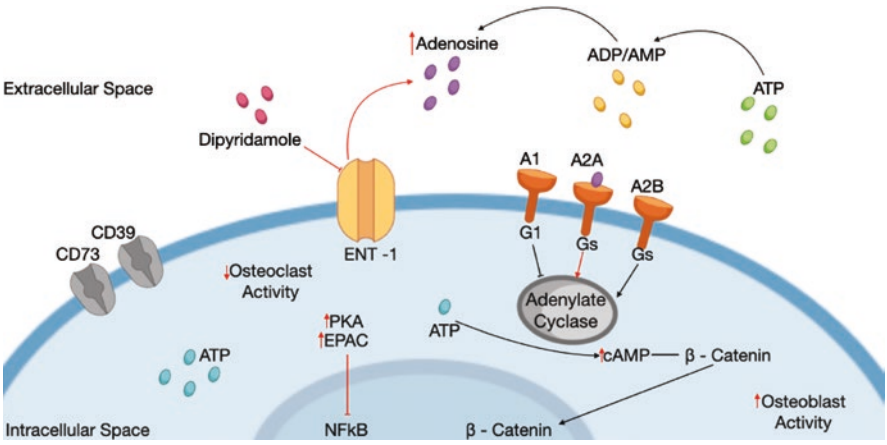

Fig. 16.2 Schematic depicting how adenosine receptor activation alters osteoclast and osteoblast activity. (Adapted from Lopez CD, Witek L, Torroni A, Flores RL, Demissie DB, Young S, et al. The role of 3D printing in treating craniomaxillofacial congenital anomalies. Birth Defects Res. 2018;110(13):1055–64)

use and has already been established as a drug in cardiac stress testing and antiplatelet therapy [37–39]. DIPY, an adenosine A_{2A} receptor indirect agonist, functions through type 1 equilibrative nucleoside transporter (ENT1) to block the reuptake of adenosine into cells causing extracellular accumulation (Fig. 16.2). With the hypothesis that DIPY can enhance bone formation while avoiding the common side effects of rhBMP-2, several tissue engineering strategies have been developed to treat critical-sized defects in immature and mature skeletal models.

Tissue Engineering Strategies: Evidence in a Small Translational Model

Research shows that bioactive ceramic scaffolds can be used to fill critically sized segmental defects and bridge defects with newly regenerated bone as early as 8 weeks in vivo. Furthermore, simultaneous scaffold degradation with bone formation and remodeling has been observed over 6 months [20]. In vivo studies have also enabled important insights into the role of adenosine indirect agonists on bone regeneration. To test the hypothesis that DIPY enhances bone regenerative capabilities of already osseoconductive ceramic 3DP constructs, β-TCP scaffolds were utilized in critical-sized calvarial defects in a A_{2A} knockout (KO) murine model [33] (Fig. 16.3). The bone regenerative capacity of DIPY was leveraged via local delivery to the defect site, thereby avoiding systemic effects while simplifying release kinetics [4]. Significantly increased bone formation was recorded for the scaffold group loaded with DIPY prior to implantation, when compared to the experimental group without the bioactive molecule.

A_{2A} receptor activation was determined to be a critical mechanism of action for bone as A_{2A} receptor knockouts failed to regenerate the cranial bone defects. Conversely, the control groups showed favorable healing, thereby highlighting the role the A_{2A} receptor plays in bone regeneration [40]. While 3DP scaffolds composed of β-TCP alone can restore bone defects, the addition of DIPY significantly increases osteogenic potential. Loading a 3D-printed (3DP) bioactive ceramic scaffold that serves as a carrier of an osseoinductive molecule like DIPY has paved the way for new tissue engineering strategies [41–43]. Research has since been conducted making extensive use of DIPY as an osseoinductive coating on fit-and-fill 3DP β-TCP scaffolds to treat critically sized defects induced in the calvaria, cleft, and mandible of translational models at multiple length scales.

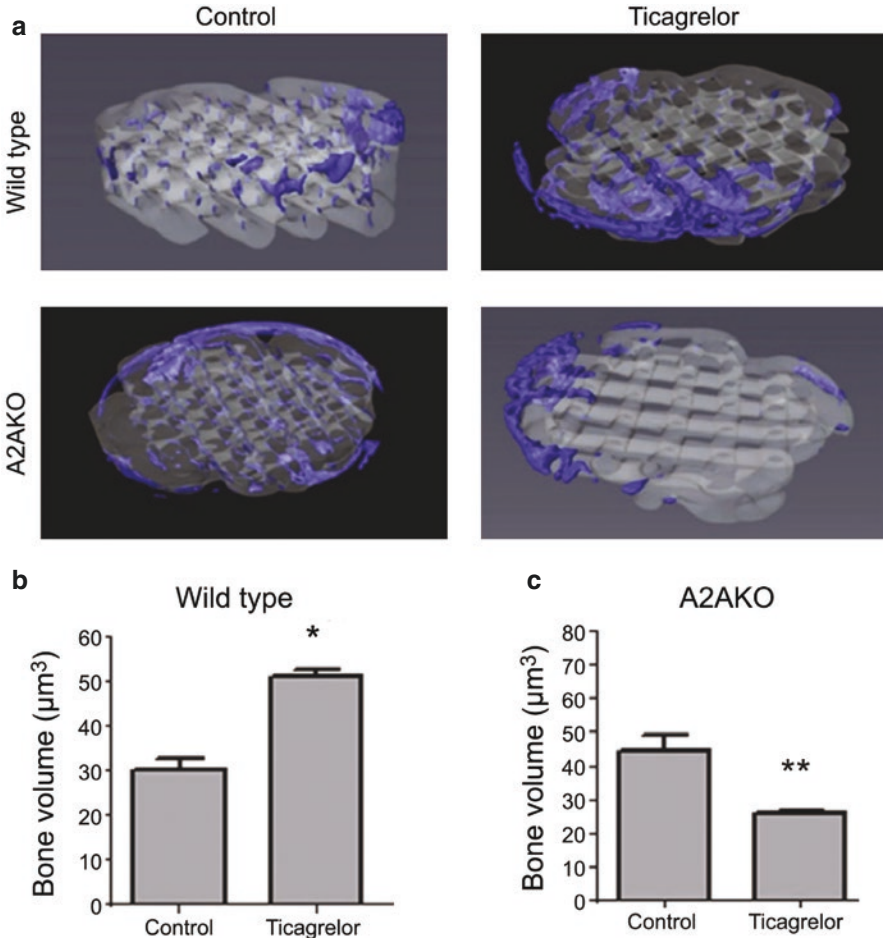

Fig. 16.3 (**a**) Volumetric reconstruction of bone and scaffold of the collagen-coated scaffold for both wild-type and A2A KO groups. Volume of new bone formation within the scaffolds at the site of trephination for (**b**) wild-type and (**c**) A2A KO groups. (Data presented as mean ± SEM). (Reproduced with permission from Mediero A, Wilder T, Reddy VS, Cheng Q, Tovar N, Coelho PG, et al. Ticagrelor regulates osteoblast and osteoclast function and promotes bone formation in vivo via an adenosine-dependent mechanism. FASEB J. 2016;30(11):3887–900)

Preclinical Translational Models

Skeletally Mature Translational Models

Murine models used in previous studies posed a concern during the quantitative and qualitative analysis of the effect of DIPY. Specifically, no attempt was made to isolate the effect of DIPY on different bone healing tissue contributors, specifically the

bone defect margin, dura, and pericranium, due to the model's constraints in size [33, 34]. Alternatively, a larger preclinical sheep model was selected for implantation of scaffolds designed with a cap (a solid barrier on the ectocortical side) to minimize the infiltration of pericranium while allowing for contact between the dura and an open, porous, lattice-based interior scaffold structure [34]. 3DP ceramic scaffolds comprised of 100% β-TCP were printed for inlay reconstruction of a surgically induced calvarial defect (Fig. 16.4). Specifically, custom 3DP scaffolds with lattice-based porosity were designed and printed such that the lattice structure faced toward the dural surface. Scaffolds were either augmented only with collagen,

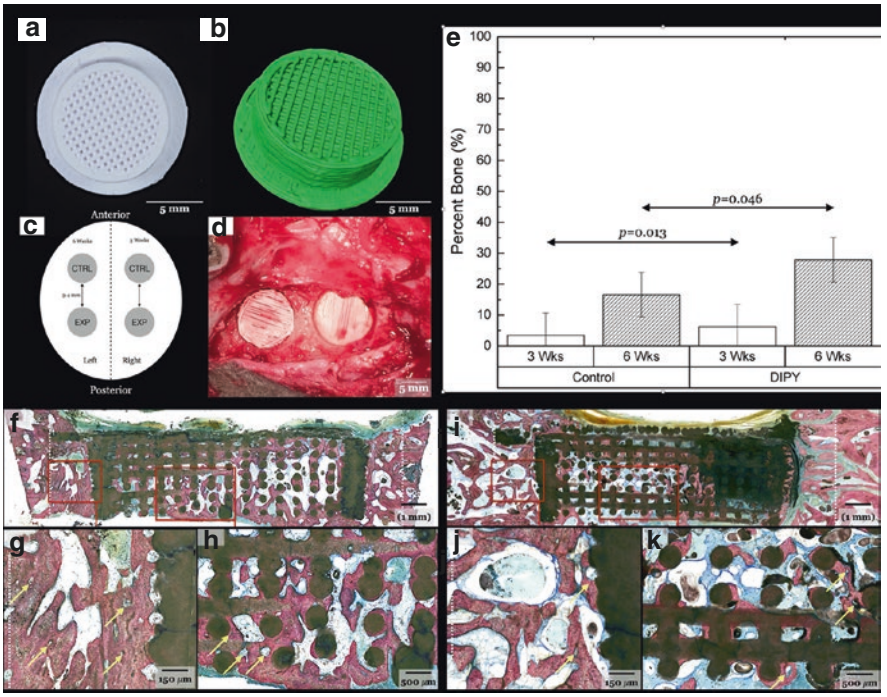

Fig. 16.4 (**a**) Inferior surface of the scaffold, (**b**) 3D reconstruction of the scaffold created using Amira 6.3 software (Visage Imaging GmbH, Berlin, Germany), (**c**) schematic representation of experimental design, (**d**) intraoperative photograph showing scaffold placement, (**e**) graph depicting the percentage of bone formation (error bars indicate 95% confidence intervals), (**f**) representative histologic image from animals in the control group at the 6-week time point, (**g**) magnification of abundant bone growth between the defect margin and wall of the scaffold with a primary osteon highlighted (yellow arrow), (**h**) angiogenesis (green arrows), (**i**) representative histologic image from animals in the DIPY group at the 6-week time point, (**j**) close-up depicting significant bony infill within the space between the defect margin and wall of the scaffold, with several osteons highlighted (yellow arrows) that provide evidence of lamellar reorganization, (**k**) angiogenesis and osteon development is evident (green arrows) and more prevalent in the DIPY group. (Reproduced with permission from Bekisz JM, Flores RL, Witek L, Lopez CD, Runyan CM, Torroni A, et al. Dipyridamole enhances osteogenesis of three-dimensionally printed bioactive ceramic scaffolds in calvarial defects. J Craniomaxillofac Surg. 2018;46(2):237–44)

which served as the control group or coated with collagen and then subsequently immersed in a 100 μM concentration DIPY solution. Two ipsilateral 11-mm calvarial defects were induced in sheep ($n = 5$) with trephines. Defects were filled with either a control or a DIPY-augmented scaffold, and the surgery was repeated on the contralateral side after 3 weeks. Following euthanasia, defects were evaluated through microCT and histomorphometric analysis for bone, scaffold, and soft tissue quantification within the defect. No histologic evidence of ectopic bone formation or inflammation was observed within the defects. Significantly higher osteogenesis was seen in DIPY-coated scaffolds compared to controls both at the 3-week ($p = 0.013$) and 6-week time points ($p = 0.046$) [34]. Furthermore, the most significant difference in results pertaining to bone regeneration was observed centrally within the interface between the 3DPBC scaffold and the dura mater, with a bone formation increase of ~85% when compared to control scaffolds at the 6-week time point.

In studies employing 3DP β-TCP scaffolds in load-bearing applications, the regenerative capacity of bioceramic scaffolds has yielded favorable results. In one such study, full-thickness, unilateral defects were induced in skeletally mature New Zealand White rabbits (NZWR) at the segmental mandibular body. β-TCP scaffolds demonstrated bone regeneration at 8 weeks in vivo [44] (Fig. 16.5). Scaffolds were seen to bridge the entire defect span despite the presence of physiological loading during masticatory function. Intramembranous-like healing was observed with vascularized woven bone formation around the scaffold indicating close contact. While good outcomes were observed in studies utilizing skeletally mature models, the challenges for regenerating skeletally immature bone are much different. For example, an alveolar cleft defect of the primary palate creates structural instability of the maxillary arch that could lead to an inability to support tooth eruption and cause facial asymmetry [19]. Current tissue engineering approaches must also be modified by considering the constraints of a growing maxillofacial skeleton. Thus, alternative therapies must be explored and employed such that premature suture fusion is not induced.

Skeletally Immature Translational Model

In scenarios involving cleft palate reconstruction in pediatric patients, autologous bone graft from the calvaria, iliac crest, and costal cartilage is limited by the volume and shape of harvestable bone, donor site morbidity, and in some instances a risk of infection. The ideal pediatric bone replacement would effectively fit and fill the defect site and restore structure and function while preserving harmonious growth. To test this hypothesis, a study was conducted in NZWR where unilateral 3.5 mm × 3.5 mm, full-thickness defects were created in the maxilla to simulate an alveolar cleft [45]. Defects were treated with custom 3D-printed scaffolds coated with bovine type 1 collagen and augmented with either 100, 1000, or 10,000 μM DIPY. Euthanasia at the 8-week time point revealed dose-dependent bone

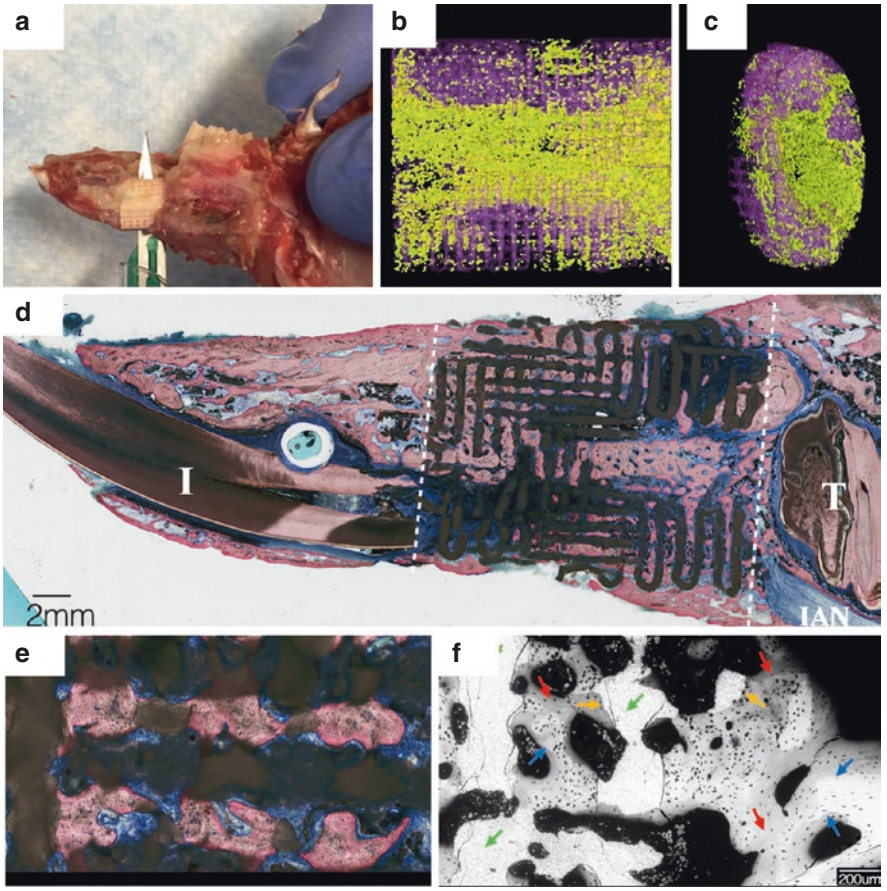

Fig. 16.5 (**a**) Scaffold integration with rabbit mandible, (**b**) lengthwise 3D reconstruction of scaffold, (**c**) end of scaffold with bony infiltration of lumen (scaffold in purple, bone in yellow), (**d**) sagittal histologic slice of scaffold in continuity with rabbit mandible, (**e**) high magnification from (**d**) demonstrating porous ingrowth, and highly cellular and vascularized woven bone structure, as well as newer, organized lamellar bone formation depicted by arrows. I, incisor; T, tooth; IAN, inferior alveolar nerve (color version of figure is available online). (**f**) Electron microscopy depicting scaffold struts (green arrows) and new bone formation throughout scaffold interstices (red arrows). New woven bone is seen filling sites of scaffold degradation (yellow arrows) and regions of lamellar reorganization juxtaposed with immature woven bone are evident (blue arrows, lamellar as brighter bone, woven is darker). (Reproduced with permission from Lopez CD, Diaz-Siso JR, Witek L, Bekisz JM, Cronstein BN, Torroni A, et al. Three-dimensionally printed bioactive ceramic scaffold osseoconduction across critical-sized mandibular defects. Journal of Surgical Research. 2018;223:115–22)

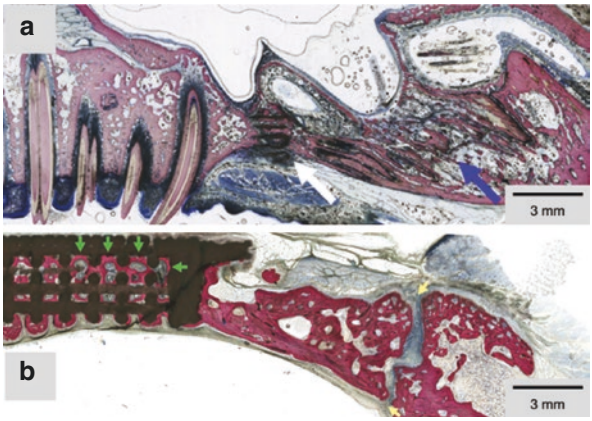

Fig. 16.6 (**a**) Alveolar cleft with scaffold at 8 weeks. Scaffold (black) lattice with bone growth (pink). Suture patency is noted as well in lower magnification (blue arrow) and (**b**) cranial sutures patent (yellow arrows) at 8 weeks evident with new bone growth in and around scaffold lattice structure (green arrows) [45, 46]

regeneration with no evidence of maxillary suture fusion (Fig. 16.6a). Regenerated bone density was increased compared to native contralateral unoperated bone. The long-term analysis revealed that there was substantial scaffold resorption at 24 weeks (6 months) relative to the 8-week time point. Newly regenerated bone using the 3DP scaffolds was seen to be analogous to the positive control animals, treated with autologous bone grafts, with no signs of asymmetry, ectopic bone growth, or morbidity. Furthermore, alveolar bone tissue was seen to ultimately remodel similar to native bone density without detriment to function when given enough time. Similarly, in an 8-week bilateral calvarial defect study involving NZWR, scaffold-induced bone growth was statistically greater than bone growth in empty defects ($p = 0.02$). Histologic analysis revealed patent calvarial sutures with no ectopic bone formation, among all (100, 1000, and 10,000 μM) DIPY concentrations [46] (Fig. 16.6b).

While the previously conducted studies have provided foundational evidence of effectiveness of 3DP β-TCP scaffolds in regenerating pediatric craniofacial defects, pediatric clinical applications would require successful implementation in a large, preclinical, translational animal model (e.g., swine). A recent study conducted on 6-week-old Göttingen minipigs served as an excellent pediatric preclinical animal model due to similarities to human bone morphology, regeneration, and wound healing [47, 48]. Unilateral calvarial defects (~1.4 cm) were created. Two groups of animals were implanted with scaffolds with or without a cap (both groups coated

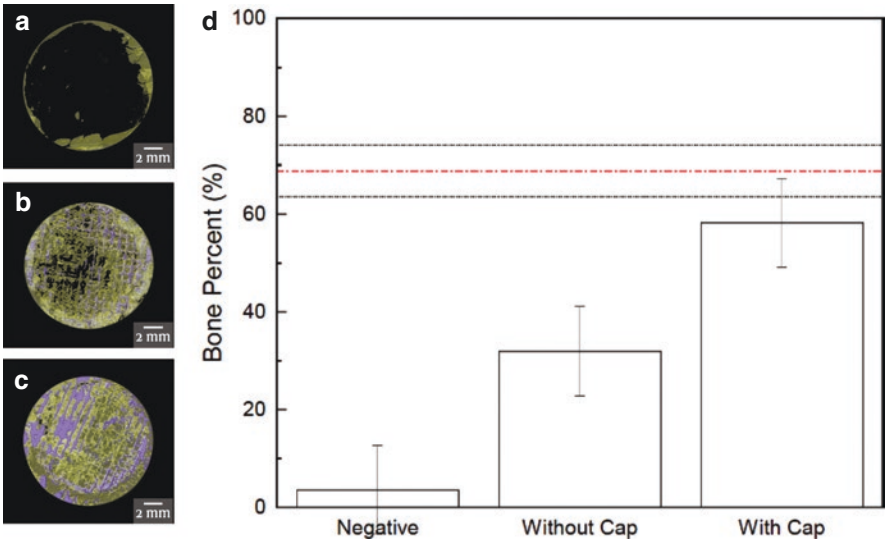

Fig. 16.7 3D reconstruction of the bone (yellow) and remaining scaffold (purple) in the defect site after 12 weeks of healing in a (**a**) negative control, (**b**) a defect that had been filled with a scaffold without a cap, (**c**) a defect that had been filled with a scaffold with a cap. (**d**) Bar graph presenting the mean (±95% CI) of bone that filled the defect sites in each group after 12 weeks of healing compared to the average bone density of native bone (red line). The horizontal dashed red line denotes the mean with corresponding 95% CI shown by the black horizontal lines

with 1000 μM DIPY), while a third group served as the negative control (no scaffold) (Figs. 16.7a and 16.8a). Animals were euthanized 12 weeks postoperatively. Defects repaired with scaffolds with caps yielded a significantly higher bone volume fraction (Fig. 16.7d) compared to defects repaired without caps ($p \leq 0.001$) (Figs. 16.7b, c, 16.8b, b.1, c, c.1).

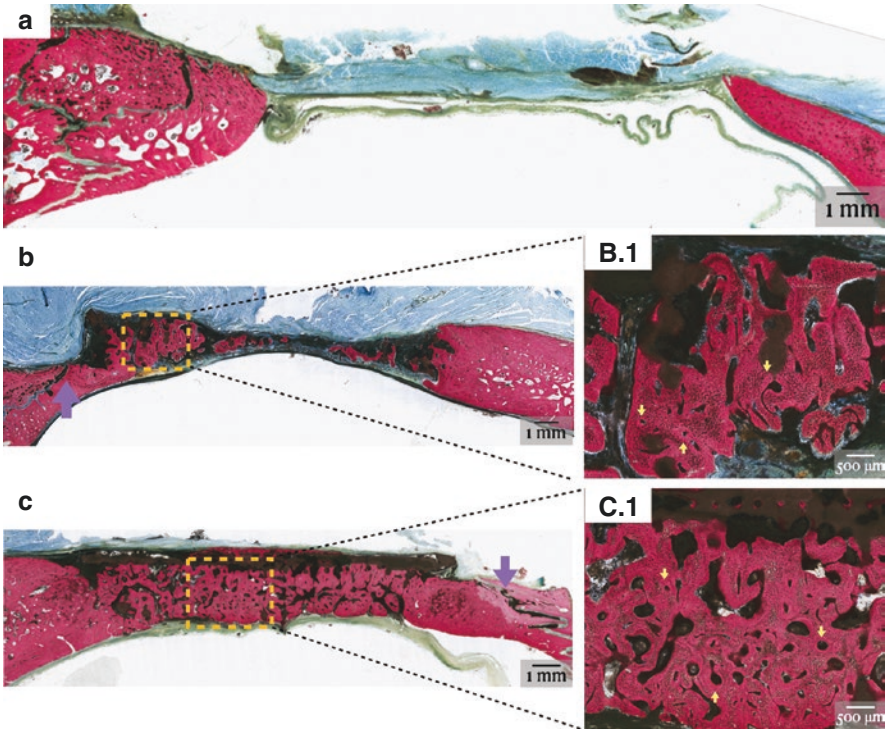

Fig. 16.8 Nondecalcified histologic sections of a (**a**) negative control after 12 weeks of healing. No bridging bone was seen across any of the unfilled defect sites, (**b**) defect filled with a scaffold that that did not contain a cap after 12 weeks of healing. Vascularized woven and lamellar bone formed throughout the defect site and cranial sutures remained patent (purple arrow). (**b.1**) Areas of mature, organized bone (yellow arrows) can be seen in the higher magnified portion of the slide. (**c**) Defect filled with a scaffold that included a cap after 12 weeks of healing. Vascularized woven and lamellar bone formed throughout the defect site and cranial sutures remained patent (purple arrow). (**c.1**) Areas of mature, organized bone (yellow arrows) can be seen in the higher magnified portion of the slide

Future Outlook

The field of CMF surgery has evolved from its sole purpose of treating a disease. With technological advancements in the field where new techniques and materials are continuously being developed, there has been an evolving need for innovative and comprehensive surgical care. To enable such advancements to proceed from bench to bedside deployment, a robust understanding of regenerative medicine and materials along with excellent surgical judgment is required. In the field of reconstructive surgery and more specifically the field of CMF, limited volume or poor bone quality has been a factor, which has warranted further research for alternatives. 3DP of porous, bioactive, and biocompatible CaP ceramic scaffolds thus far

has shown excellent results in repairing critically sized bony defects. 3DP implants have not only shown an ability to perform the desired function of bone healing but have also induced favorable responses in the presence of physiological loads. Significant bone healing has hence been recorded in anatomic locations such as the mandible. Furthermore, the combination of 3DP scaffolds and $A_{2A}R$ activation has proven fruitful in augmenting bone growth in calvarial defects in large translational models without any changes to suture biology. Similar responses have been observed in alveolar cleft and calvarial defects in the growing craniofacial skeleton. With these advancements, however, come several challenges which surgeons should be aware of, in addition to fully understanding the principle components of tissue engineering: scaffolds, bioactive agents, and stem cell therapies. While scaffolds and pharmaceutical bioactive molecules have been explored and have shown favorable results, clinical deployment of stem cell therapies has not yet demonstrated desired outcomes [49, 50]. As such, regulatory concerns pose a major challenge in the deployment of some of these techniques for clinical trials. Nevertheless, the relative ease of 3DP, abundant material availability, and most importantly, proven, complete re-establishment of form and function at skeletal defect sites warrant further investigation, especially through direct translation in patients.

Acknowledgments The work presented in this chapter was supported by NIH/NIAMS (MPI-Cronstein, Coelho) R01AR068593, R01AR068593-S1, NIH/NICHD (MPI-Coelho, Flores, Crosntein, and Witek) R21R33HD090664, DoD (MPI-Rodriguez, Coelho) W81XWH-16-1-0772, and an Osteo Science Foundation Peter Geistlich Research Award (MPI-Coelho, Kasper, Young, and Witek). Dr. Coelho is a co-inventor of the 3D-printing technology presented in this chapter (Patent #: US20150150681A1).

References

1. Lanza RP. Principles of tissue engineering. 5th ed. London: Academic Press; 2020.
2. Seper L, Piffkó J, Joos U, Meyer U. Treatment of fractures of the atrophic mandible in the elderly. J Am Geriatr Soc. 2004;52(9):1583–4.
3. American Society of Plastic Surgeons. 2020 Plastic surgery statistics. Arlington Heights, IL: American Society of Plastic Surgeons; 2020. https://www.plasticsurgery.org/documents/News/Statistics/2020/plastic-surgery-statistics-full-report-2020.pdf.
4. Witek L, Colon RR, Wang MM, Torroni A, Young S, Melville J, et al. 24 - Tissue-engineered alloplastic scaffolds for reconstruction of alveolar defects. In: Mozafari M, Sefat F, Atala A, editors. Handbook of tissue engineering scaffolds, vol. 1. New Delhi: Woodhead Publishing; 2019. p. 505–20.
5. Lopez CD, Witek L, Torroni A, Flores RL, Demissie DB, Young S, et al. The role of 3D printing in treating craniomaxillofacial congenital anomalies. Birth Defects Res. 2018;110(13):1055–64.
6. Wang MM, Flores RL, Witek L, Torroni A, Ibrahim A, Wang Z, et al. Dipyridamole-loaded 3D-printed bioceramic scaffolds stimulate pediatric bone regeneration in vivo without disruption of craniofacial growth through facial maturity. Sci Rep. 2019;9(1):18439.
7. Lopez CD, Diaz-Siso JR, Witek L, Bekisz JM, Gil LF, Cronstein BN, et al. Dipyridamole augments three-dimensionally printed bioactive ceramic scaffolds to regenerate craniofacial bone. Plast Reconstr Surg. 2019;143(5):1408–19.

8. Gimbel M, Ashley RK, Sisodia M, Gabbay JS, Wasson KL, Heller J, et al. Repair of alveolar cleft defects: reduced morbidity with bone marrow stem cells in a resorbable matrix. J Craniofac Surg. 2007;18(4):895.
9. Wang RR, Andres CJ, Wang RR, Andres CJ. Hemifacial microsomia and treatment options for auricular replacement: a review of the literature. J Prosthet Dent. 1999;82(2):197–204.
10. Plomp RG, van Lieshout MJS, Joosten KFM, Wolvius EB, van der Schroeff MP, Versnel SL, et al. Treacher Collins Syndrome: a systematic review of evidence-based treatment and recommendations. Plast Reconstr Surg. 2016;137(1):191.
11. Fan KL, Federico C, Kawamoto HK, Bradley JP. Optimizing the timing and technique of Treacher Collins orbital malar reconstruction. J Craniofac Surg. 2012;23(7 Suppl 1):2033–7.
12. Shen C, et al. Three-dimensional printing for craniofacial bone tissue engineering. Tissue Eng A. 2020;26(23–24):1303–11.
13. Dawood A, Marti Marti B, Sauret-Jackson V, Darwood A. 3D printing in dentistry. Br Dent J. 2015;219(11):521–9.
14. Baker MI, Eberhardt AW, Martin DM, McGwin G, Lemons JE. Bone properties surrounding hydroxyapatite-coated custom osseous integrated dental implants. J Biomed Mater Res B Appl Biomater. 2010;95(1):218–24.
15. Ducheyne P, De Groot K. In vivo surface activity of a hydroxyapatite alveolar bone substitute. J Biomed Mater Res. 1981;15(3):441–5.
16. Ducheyne P, Hench LL, Kagan A II, Martens M, Bursens A, Mulier JC. Effect of hydroxyapatite impregnation on skeletal bonding of porous coated implants. J Biomed Mater Res. 1980;14(3):225–37.
17. Ducheyne P, Van Raemdonck W, Heughebaert JC, Heughebaert M. Structural analysis of hydroxyapatite coatings on titanium. Biomaterials. 1986;7(2):97–103.
18. Duheyne P, Beight J, Cuckler J, Evans B, Radin S. Effect of calcium phosphate coating characteristics on early post-operative bone tissue ingrowth. Biomaterials. 1990;11(8):531–40.
19. Lopez CD, Witek L, Flores RL, Torroni A, Rodriguez ED, Cronstein BN, et al. 3D printing and adenosine receptor activation for craniomaxillofacial regeneration. In: Melville JC, Shum JW, Young S, Wong ME, editors. Regenerative strategies for maxillary and mandibular reconstruction: a practical guide. Cham: Springer International Publishing; 2019. p. 255–67.
20. Tovar N, Witek L, Atria P, Sobieraj M, Bowers M, Lopez CD, et al. Form and functional repair of long bone using 3D-printed bioactive scaffolds. J Tissue Eng Regen Med. 2018;12(9):1986–99.
21. Witek L, Smay J, Silva NRFA, Guda T, Ong JL, Coelho PG. Sintering effects on chemical and physical properties of bioactive ceramics. J Adv Ceram. 2013;2(3):274–84.
22. Moore WR, Graves SE, Bain GI. Synthetic bone graft substitutes. ANZ J Surg. 2001;71(6):354–61.
23. Shen C, Wang MM, Witek L, Tovar N, Cronstein BN, Torroni A, et al. Transforming the degradation rate of β-tricalcium phosphate bone replacement using 3-dimensional printing. Ann Plast Surg. 2021;87(6):e153.
24. Smay JE, Lewis JA. Solid free-form fabrication of 3-D ceramic structures. Ceramics and composites processing methods. 1st ed. Hoboken, NJ: Wiley; 2012. p. 459–84.
25. Melville JC, Nassari NN, Hanna IA, Shum JW, Wong ME, Young S. Immediate transoral allogeneic bone grafting for large mandibular defects. Less morbidity, more bone. A paradigm in benign tumor mandibular reconstruction? J Oral Maxillofac Surg. 2017;75(4):828–38.
26. Melville JC, Shum JW, Young S, Wong ME. Regenerative strategies for maxillary and mandibular reconstruction: a practical guide. New York, NY: Springer; 2019.
27. Jäger M, Herten M, Fochtmann U, Fischer J, Hernigou P, Zilkens C, et al. Bridging the gap: bone marrow aspiration concentrate reduces autologous bone grafting in osseous defects. J Orthop Res. 2011;29(2):173–80.
28. Melville JC, Tursun R, Green JM III, Marx RE. Reconstruction of a post-traumatic maxillary ridge using a radial forearm free flap and immediate tissue engineering (bone morphogenetic

protein, bone marrow aspirate concentrate, and cortical-cancellous bone): case report. J Oral Maxillofac Surg. 2017;75(2):438.e1–6.
29. Costa MA, Barbosa A, Neto E, Sá-e-Sousa A, Freitas R, Neves JM, et al. On the role of subtype selective adenosine receptor agonists during proliferation and osteogenic differentiation of human primary bone marrow stromal cells. J Cell Physiol. 2011;226(5):1353–66.
30. Mediero A, Cronstein BN. Adenosine and bone metabolism. Trends Endocrinol Metab. 2013;24(6):290–300.
31. Mediero A, Frenkel SR, Wilder T, He W, Mazumder A, Cronstein BN. Adenosine A2A receptor activation prevents wear particle-induced osteolysis. Sci Transl Med. 2012;4(135):135ra65.
32. Mediero A, Wilder T, Perez-Aso M, Cronstein BN. Direct or indirect stimulation of adenosine A2A receptors enhances bone regeneration as well as bone morphogenetic protein-2. FASEB J. 2015;29(4):1577–90.
33. Mediero A, Wilder T, Reddy VS, Cheng Q, Tovar N, Coelho PG, et al. Ticagrelor regulates osteoblast and osteoclast function and promotes bone formation in vivo via an adenosine-dependent mechanism. FASEB J. 2016;30(11):3887–900.
34. Bekisz JM, Flores RL, Witek L, Lopez CD, Runyan CM, Torroni A, et al. Dipyridamole enhances osteogenesis of three-dimensionally printed bioactive ceramic scaffolds in calvarial defects. J Craniomaxillofac Surg. 2018;46(2):237–44.
35. Martin C, Leone M, Viviand X, Ayem ML, Guieu R. High adenosine plasma concentration as a prognostic index for outcome in patients with septic shock. Crit Care Med. 2000;28(9):3198–202.
36. Cronstein BN, Kramer SB, Weissmann G, Hirschhorn R. A new physiological function for adenosine: regulation of superoxide anion production. Trans Assoc Am Phys. 1983;96:384–91.
37. Fitz Gerald GA. Dipyridamole. N Engl J Med. 1987;316(20):1247–57.
38. Patrono C, Coller B, Dalen JE, Fuster V, Gent M, Harker LA, et al. Platelet-active drugs: the relationships among dose, effectiveness, and side effects. Chest. 1998;114(5 Suppl):470s–88s.
39. Monagle P, Chan AK, Goldenberg NA, Ichord RN, Journeycake JM, Nowak-Göttl U, et al. Antithrombotic therapy in neonates and children: antithrombotic therapy and prevention of thrombosis: American College of Chest Physicians Evidence-Based Clinical Practice Guidelines. Chest. 2012;141(2):e737S–801S.
40. Ishack S, Mediero A, Wilder T, Ricci JL, Cronstein BN. Bone regeneration in critical bone defects using three-dimensionally printed β-tricalcium phosphate/hydroxyapatite scaffolds is enhanced by coating scaffolds with either dipyridamole or BMP-2. J Biomed Mater Res B Appl Biomater. 2017;105(2):366–75.
41. Carragee EJ, Hurwitz EL, Weiner BK. A critical review of recombinant human bone morphogenetic protein-2 trials in spinal surgery: emerging safety concerns and lessons learned. Spine J. 2011;11(6):471–91.
42. Spiro AS, Beil FT, Baranowsky A, Barvencik F, Schilling AF, Nguyen K, et al. BMP-7-induced ectopic bone formation and fracture healing is impaired by systemic NSAID application in C57BL/6-mice. J Orthop Res. 2010;28(6):785–91.
43. Kinsella CR, Cray JJ, Durham EL, Burrows AM, Vecchione L, Smith DM, et al. Recombinant human bone morphogenetic protein-2-induced craniosynostosis and growth restriction in the immature skeleton. Plast Reconstr Surg. 2011;127(3):1173–81.
44. Lopez CD, Diaz-Siso JR, Witek L, Bekisz JM, Cronstein BN, Torroni A, et al. Three dimensionally printed bioactive ceramic scaffold osseo conduction across critical-sized mandibular defects. J Surg Res. 2018;223:115–22.
45. Lopez CD, Coelho PG, Witek L, Torroni A, Greenberg MI, Cuadrado DL, et al. Regeneration of a pediatric alveolar cleft model using three-dimensionally printed bioceramic scaffolds and osteogenic agents: comparison of dipyridamole and rhBMP-2. Plast Reconstr Surg. 2019;144(2):358.
46. Maliha SG, Lopez CD, Coelho PG, Witek L, Cox M, Meskin A, et al. Bone Tissue engineering in the growing calvaria using dipyridamole-coated, three-dimensionally-printed bioceramic

scaffolds: construct optimization and effects on cranial suture patency. Plast Reconstr Surg. 2020;145(2):337e–47e.
47. McGovern JA, Griffin M, Hutmacher DW. Animal models for bone tissue engineering and modelling disease. Dis Model Mech. 2018;11(4):dmm033084.
48. Li Y, Chen SK, Li L, Qin L, Wang XL, Lai YX. Bone defect animal models for testing efficacy of bone substitute biomaterials. J Orthop Transl. 2015;3(3):95–104.
49. Weinand C, Neville CM, Weinberg E, Tabata Y, Vacanti JP. Optimizing biomaterials for tissue engineering human bone using mesenchymal stem cells. Plast Reconstr Surg. 2016;137(3):854–63.
50. Cooper GM, Miller ED, Decesare GE, Usas A, Lensie EL, Bykowski MR, et al. Inkjet-based biopatterning of bone morphogenetic protein-2 to spatially control calvarial bone formation. Tissue Eng Part A. 2010;16(5):1749–59.